

Azimuthally asymmetric ring current as a function of D_{st} and solar wind conditions

Y. P. Maltsev and A. A. Ostapenko

Polar Geophysical Institute, Apatity, Murmansk region, 184209, Russia

Received: 29 October 2003 – Revised: 10 March 2004 – Accepted: 8 April 2004 – Published: 7 September 2004

Abstract. Based on magnetic data, spatial distribution of the westward ring current flowing at $|z| < 3 R_E$ has been found under five levels of D_{st} , five levels of the interplanetary magnetic field (IMF) z component, and five levels of the solar wind dynamic pressure P_{sw} . The maximum of the current is located near midnight at distances 5 to 7 R_E . The magnitude of the nightside and dayside parts of the westward current at distances from 4 to 9 R_E can be approximated as $I_{\text{night}} = 1.75 - 0.041 D_{st}$, $I_{\text{noon}} = 0.22 - 0.013 D_{st}$, where the current is in MA. The relation of the nightside current to the solar wind parameters can be expressed as $I_{\text{night}} = 1.45 - 0.20 B_s \text{IMF} + 0.32 P_{sw}$, where $B_s \text{IMF}$ is the IMF southward component. The dayside ring current poorly correlates with the solar wind parameters.

Key words. Magnetospheric physics (current systems; solar wind-magnetosphere interactions; storms and substorms)

1 Introduction

The ring electric current flows in the stable trapping region at distances of less than 10 R_E (R_E is the Earth's radius). The ring current is carried predominantly by protons with energy of 10–100 keV. During strong magnetic storms the ions of O^+ also contribute to the ring current (Daglis et al., 1999).

Strong azimuthal asymmetry of the ring current was found by Iijima et al. (1990) from magnetic measurements on board AMPTE CCE for a prolonged disturbed period ($2 < K_p < 6$, $-20 > D_{st} > -70$). The current at distance from 4 to 8.8 R_E in the nightside appeared to be 2–3 times greater than in the dayside.

There are a lot of case studies of energetic particles in the ring current region (Frank, 1967; Smith and Hoffman, 1973; Lui et al., 1987; Hamilton et al., 1988; Spence et al., 1989; Korth and Friedel, 1997; Kalegaev et al., 1998; Dremukhina et al., 1999). Statistical studies are not so numerous. Lui and Hamilton (1992) obtained plasma pressure radial pro-

files from $L=2$ to $L=9$ at noon and at midnight for quiet conditions. De Michelis et al. (1999), using AMPTE CCE data, have built energetic plasma profiles in four LT sectors for two AE ranges. The profiles appeared to be independent either of LT or AE . The ring current calculated from the formula

$$[\mathbf{j} \times \mathbf{B}] = \nabla_{\perp} p_{\perp} + (p_{\parallel} - p_{\perp}) \left(\frac{\mathbf{B}}{B} \nabla \right) \frac{\mathbf{B}}{B}$$

appeared to be several times stronger at midnight than at noon.

Greenspan and Hamilton (2000) utilized the particle measurements during 80 storms for checking the Dessler-Parker-Sckopke (DPS) formula, which relates the total energy content of the trapped particles to geomagnetic storm time depression D_{st} . In the nightside the energy content at distances $2 < L < 7$ appeared to agree well with the DPS formula, whereas in the daytime sector no essential correlation was revealed between the D_{st} variation and energy content.

Turner et al. (2001), in verifying the DPS formula by Polar satellite data, found that under weak storm activity trapped particles contribute $\sim 75\%$ to D_{st} . Under $D_{st} = -100$ nT the contribution of particles in the dayside drops down to 40%.

In this paper we study the ring current from magnetic data. Both symmetrical and azimuthally asymmetric ring current components will be examined as functions of D_{st} and solar wind parameters. Our results will be compared with the predictions of the models T96 (Tsyganenko, 1996) and T02 (Tsyganenko, 2002a, b).

2 Data processing technique

The database of Fairfield et al. (1994) contains about 70 000 three-component external magnetic field measurements performed by 11 satellites at distances from 3 to 60 R_E for 20 years. For all data points D_{st} values are available. For about 60% of data points there are hourly values of solar wind parameters. We divided the whole data set into five ranges: first relative to D_{st} values, then relative to $B_z \text{IMF}$ values, finally relative to solar wind dynamic pressure $P_{sw} = m n V^2$, where m , n , and V are the proton mass,

Table 1. D_{St} and solar wind parameters inside each subset studied.

Range	D_{St} , nT	P_{sw} , nPa	B_z IMF, nT	V , km/s	n , cm^{-3}	Number of data
$D_{St} \geq 0$	7	2.5	1.0	365	11.4	3199
$-15 \leq D_{St} < 0$	-8	2.0	0.6	402	7.8	4842
$-30 \leq D_{St} < -15$	-23	2.1	-0.2	436	7.0	2782
$-50 < D_{St} < -30$	-39	2.3	-1.5	468	6.5	1916
$D_{St} \leq -50$	-74	3.6	-2.2	500	8.8	1173
B_z IMF ≥ 3 nT	-13.5	3.1	5.4	421	10.5	1810
$1 \leq B_z$ IMF < 3 nT	-11.5	2.1	1.8	409	7.9	2048
$-1 \leq B_z$ IMF < 1 nT	-12.9	2.0	-0.1	408	7.7	2879
$-3 \leq B_z$ IMF < -1 nT	-18.4	2.2	-1.9	424	8.0	1938
B_z IMF < -3 nT	-33.1	3.0	-5.4	424	10.0	1731
$P_{sw} \leq 1.2$	-16	0.9	0.1	395	3.7	2031
$1.2 < P_{sw} < 2$	-15	1.6	0.0	409	6.3	3580
$2 \leq P_{sw} < 3$	-17	2.4	-0.2	418	9.3	2514
$3 \leq P_{sw} < 4$	-18	3.4	0.1	429	12.8	1036
$P_{sw} \geq 4$	-24	6.7	0.6	467	20.5	1219

number density, and velocity, respectively. The parameters of the subsets, as well as the number of magnetic data in each subset, are given in Table 1 for the body of data confined in the disk of $\rho < 10 R_E$, $|z| < 4 R_E$, where the coordinates are in the SM system; $\rho = (x^2 + y^2)^{1/2}$ is the cylindrical distance.

The surface electric current density inside the near-equatorial layer was calculated for each subset as

$$\mathbf{J}_\perp = \int_{-z_0}^{z_0} \mathbf{j}_\perp dz = \frac{1}{\mu_0} \oint [\mathbf{B} \times d\mathbf{l}]. \quad (1)$$

The integration contour was adopted to be a rectangle with the vertical side of $-z_0 < z < z_0$, where $z_0 = 3 R_E$ and horizontal side of $1 R_E$. We used the horizontal magnetic components B_ρ and B_φ in the layers $2 < |z| < 4 R_E$ and vertical component B_z in the layer $-3 < z < 3 R_E$. Each of the three components was sought in the following form

$$B = f_0 = f + f_1 \cos \varphi + f_2 \sin \varphi, \quad (2)$$

where φ is the longitude. The coefficients f_0 , f_1 , and f_2 were fitted by the least-squares technique inside the radial bins $\Delta\rho = 1 R_E$. The relative residual error RES was calculated from the formula

$$RES = \frac{\sum_{n=1}^N (\mathbf{B}_n^{\text{obs}} - \mathbf{B}_n^{\text{mod}})^2}{\sum_{n=1}^N (\mathbf{B}_n^{\text{obs}})^2},$$

where $\mathbf{B}_n^{\text{obs}}$ and $\mathbf{B}_n^{\text{mod}}$ are the observed and model fields in the n th observation point, N is the total number of observations. The fitting error RES in different subsets shown in Table 1 varies from ~ 20 to $\sim 40\%$. The total RES for the five D_{St} subsets is 24% in the disks of $\rho < 10 R_E$, $2 < |z| < 4 R_E$, when estimated by B_ρ and B_z magnetic components solely used for calculating the azimuthal current. The T02 model yields $RES = 28\%$ under the same conditions.

Previously we processed the data with a more straightforward technique, with the external magnetic field being running averaged in bins with horizontal sizes of $3 R_E$ and vertical sizes of $2 R_E$ (Ostapenko and Maltsev, 2003). That approach yielded similar results but with larger scattering.

3 Distribution of azimuthal currents in the magnetosphere

Distribution of the azimuthal current for five ranges of D_{St} values, five ranges of B_z IMF, and five ranges of P_{sw} is shown in Fig. 1. The currents at $\rho > 10 R_E$ are also shown; they are not very reliable though, because the SM coordinate system is hardly appropriate for these distances. One can see that the currents grow with enhancement of storm time activity, southward IMF, and solar wind dynamic pressure. Strong day-night asymmetry is evident, the nightside current density being several times greater than the dayside one. The dawn-dusk asymmetry is rather weak and does not increase with growing activity.

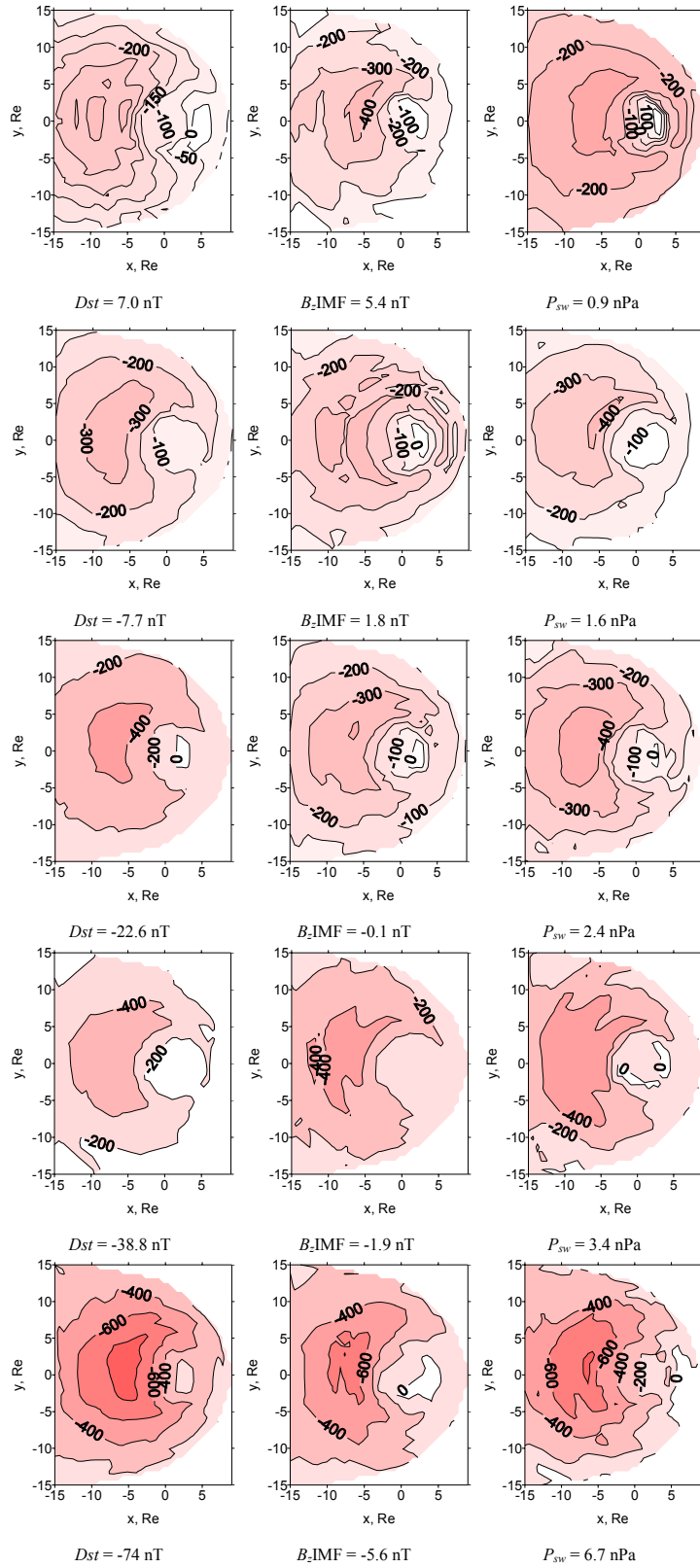


Fig. 1. Surface density (in kA/RE) of the azimuthal (eastward) component of the electric current in the sheet of $-3 < z < 3 R_E$

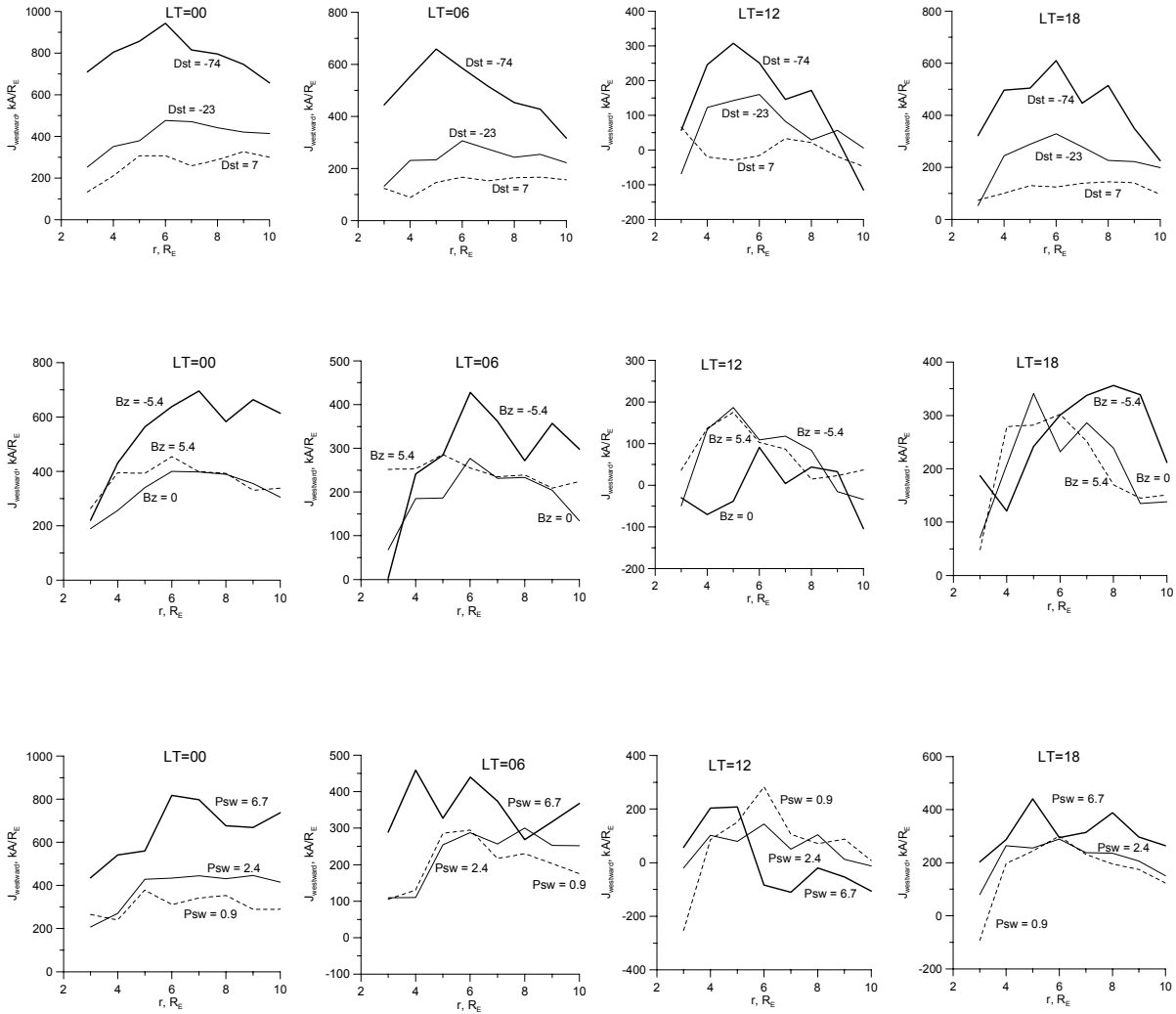


Fig. 2. Radial distribution of the westward electric current in different LT sectors under various (top) D_{st} , (middle) B_z IMF, and (bottom) P_{sw} . The thick solid lines correspond to higher activity, the dashed lines correspond to lower one.

Figure 2 shows the radial distribution of the azimuthal current surface density for four local times. The westward current dominates almost everywhere. Its radial profile has maximum at $L \approx 7$. There is no pronounced dependence of maximum location either on LT or geomagnetic activity. An eastward current is seen only in the dayside at $L=3$ under low activity.

Figure 3 shows the total westward current flowing between radial distances of 4 and 9 R_E at four local times. One can see the growth of the nightside ring current I_{night} with the D_{st} , southward IMF, and P_{sw} . A weaker relation of the dayside current on these parameters takes place, the dependence on B_s IMF and P_{sw} turned out to be inverse. The distributions in Fig. 3 are consistent with the following approximations

$$I_{night} = 1.75 - 0.041 D_{st}, \tag{3}$$

$$I_{noon} = 0.22 - 0.013 D_{st}, \tag{4}$$

$$I_{night} = 2.04 - 0.27 B_s \text{ IMF}, \tag{5}$$

$$I_{noon} = 0.63 + 0.083 B_s \text{ IMF}, \tag{6}$$

$$I_{night} = 1.60 + 0.37 P_{sw}, \tag{7}$$

$$I_{noon} = 0.68 - 0.05 P_{sw}, \tag{8}$$

where I_{night} is expressed in MA, P_{sw} in nPa, and D_{st} and B_s IMF in nT. Here B_s IMF is the IMF southward component ($B_s=0$ for $B_z>0$ and $B_s=B_z$ for $B_z<0$). The residual error of the fitting is 2% for Eqs. (4)–(7) and 35% for Eq. (8).

Since there is a correlation between B_s IMF modulus and P_{sw} , each of expressions (5)–(8) contains a dependence not on a single parameter but on both B_s IMF and P_{sw} . In order to avoid the effect of this correlation, we found the distribution of the azimuthal current in five B_z IMF ranges under P_{sw} varying in the narrow range of $1 < P_{sw} < 2$ nPa, and, oppositely in five P_{sw} ranges under $B_z > 0$. The latter condition implies that the northward IMF is not geoefficient. For these

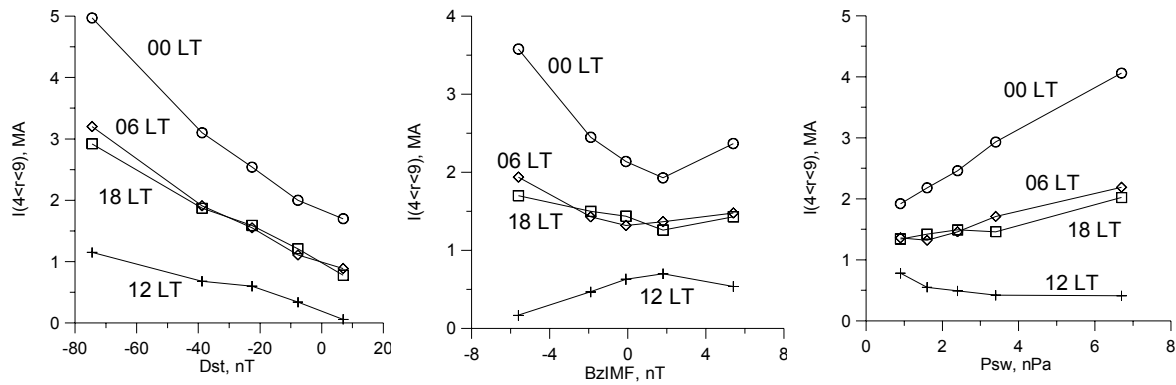


Fig. 3. Total current flowing at radial distances from 4 to $9 R_E$ versus (left) D_{st} , (middle) B_z IMF, and (right) P_{sw} in four LT sectors.

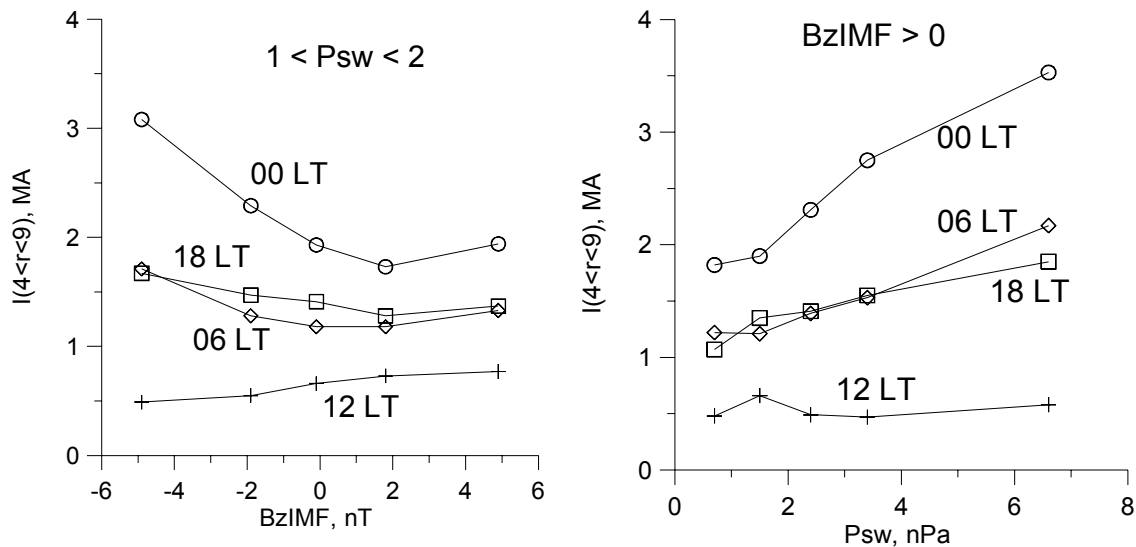


Fig. 4. Total current flowing at radial distances from 4 to $9 R_E$ vs. (left) B_z IMF in a narrow range of P_{sw} , and (right) P_{sw} under positive B_z IMF in four LT sectors.

cases the total current in four LT sectors is shown in Fig. 4. The following approximations are appropriate

$$I_{\text{night}}(1 < P_{sw} < 2) = 1.88 - 0.24 B_z \text{IMF}, \quad (9)$$

$$I_{\text{noon}}(1 < P_{sw} < 2) = 0.64 + 0.034 B_z \text{IMF}, \quad (10)$$

$$I_{\text{night}}(B_z > 0) = 1.53 + 0.31 P_{sw}, \quad (11)$$

$$I_{\text{noon}}(B_z > 0) = 0.62 - 0.015 P_{sw}. \quad (12)$$

The ten subsets utilized in obtaining expressions (9)–(12) can be considered as nearly independent, which yields a possibility to obtain the following bivariate approximation function for the nightside current

$$I_{\text{night}} = 1.45 - 0.20 B_z \text{IMF} + 0.32 P_{sw}. \quad (13)$$

The relative residual error of the fitting is 3%. We do not give the corresponding approximation for the dayside current because the error of fitting appeared to be very large, more than 60%.

One can see from expressions (3) and (13) that the relative role of the solar wind pressure and storm intensity in the nightside ring current is comparable. The standard deviations of P_{sw} , B_z IMF, and D_{st} shown in Table 1 are equal to 2.1 nPa, 1.4 nT, and 17 nT, respectively. A change of one of these parameters by a value of its standard deviation gives rise to the variation in I_{night} , which is ~ 0.7 MA for both P_{sw} and D_{st} , and ~ 0.3 MA for B_z IMF.

In the dayside the ring current is several times weaker and reveals rather a small dependence on D_{st} , B_z IMF, and P_{sw} . Under disturbed conditions and high P_{sw} , the dayside magnetopause moves closer to the Earth. Our statistical analysis can include magnetic field measurements in the magnetosheath. This may account for part of the poor correlation between the noon current and the parameters P_{sw} , D_{st} and B_z . Nevertheless, as seen from Fig. 2, the current density at all geocentric distances in the dayside is several times lower than that in the nightside.

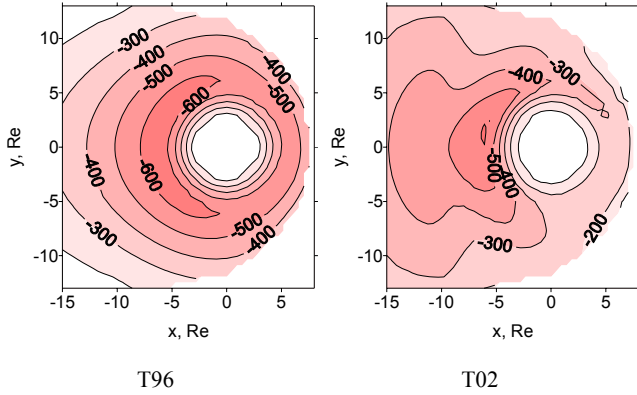


Fig. 5. Surface density of the azimuthal electric current in two models by Tsyganenko.

4 Discussion

Our results are consistent with those of Iijima et al. (1990) and De Michelis et al. (1999), who obtained the dayside ring current several times smaller than the nightside one. According to our Fig. 3, the noon current weakly depends on D_{st} and does not reveal any pronounced correlation with either B_z IMF or solar wind dynamic pressure P_{sw} .

Earlier, Greenspan and Hamilton (2000) found no essential correlation between D_{st} and the total plasma energy content in the dayside sector. On the other hand, Turner et al. (2001) obtained that the dayside particles contribute $\sim 75\%$ to D_{st} under $D_{st}=0$ and $\sim 40\%$ under $D_{st}=-100$ nT. However, the orbit of the Polar satellite, whose data they processed, was placed at $\sim 90^\circ$ to the equatorial plane, so that the satellite detected a minor fraction of trapped particles, namely, those whose pitch-angles were sufficiently small at the equator.

We conclude that the ring current near the noon can be considered as a symmetrical ring current (SRC). The nightside current at distances from 4 to $9 R_E$ consists of three parts: 1) the SRC closed in the near-equatorial inner magnetosphere, 2) partial ring current (PRC) closed to the Region 2 field-aligned currents revealed by Iijima and Potemra (1976), and 3) cross-tail current (CTC) closed to the currents on the magnetopause. Figure 3 shows that the SRC is smaller than the sum of the PRC and CTC. Our study does not allow for distinguishing between the PRC and CTC.

Let us estimate the contribution of these currents to D_{st} . A symmetrical ring current of 1 MA magnitude flowing at a distance of $6 R_E$ produces the disturbance $B_z^{rc}(0) \approx -16$ nT in the Earth's center. The corresponding ground magnetic effect is $DR = k B_z^{rc}(0) \approx -21$ nT, where $k \approx 1.3$ is due to induction currents in the Earth (Langel and Estes, 1985; Häkkinen et al., 2002). Note that the noon current presents a purely symmetrical part of the ring current, without contribution of the partial ring and cross-tail currents. Multiplying Eq. (4) by -21 we obtain the ground magnetic effect of the symmet-

rical ring current

$$DR_{SRC} = -4.6 + 0.27 D_{st}. \quad (14)$$

Thus, the contribution of the symmetrical ring current to D_{st} is 27%. This value is intermediate between the estimates of Greenspan and Hamilton (2000) and Turner et al. (2001).

Subtracting Eq. (4) from Eq. (3) we can obtain the sum of the partial ring current (PRC) and near-Earth cross-tail current (NCT)

$$I_{PRC} + I_{NCT} = 1.53 - 0.028 D_{st}. \quad (15)$$

Suppose this current flows in the nightside sector from 18:00 to 06:00 LT at a distance of $6 R_E$. Each MA of the current produces the disturbance of -8 nT in the Earth's center or $-8 \times 1.3 = 10.4$ nT on the ground surface at low latitudes. The corresponding dependence of the disturbance on D_{st} has the form

$$DR_{PRC} + DR_{NCT} = -16 + 0.29 D_{st}. \quad (16)$$

Hence, the whole contribution of the partial ring and near-Earth cross-tail currents to D_{st} is about 29%.

Strong dependence of the nightside current on the solar wind dynamic pressure P_{sw} is consistent with observations of Terasawa et al. (1997), who found that the plasma pressure in the plasma sheet is related to P_{sw} . One can expect the growth of the cross-tail current with pressure increasing. In spite of the growth of the nightside currents, their ground effect is cancelled by increasing magnetopause currents, so that D_{st} does not change practically.

The decrease of the dayside current with growing P_{sw} seems rather uncommon (we shall see further that the T02 model predicts the same relation of I_{noon} on P_{sw}). However, this peculiar result can be reasonably explained as follows. The electric current density in the equatorial plane in plasma with isotropic pressure p has the form

$$j_\varphi = \frac{1}{B} \frac{\partial p}{\partial \rho}.$$

The magnetic field B in the dayside magnetosphere grows with the solar wind dynamic pressure P_{sw} increasing. If the derivative $\partial p / \partial \rho$ grows at a smaller rate, then the current density drops. In the nightside at $x < -4 R_E$ the magnetic field in the equatorial plane decreases when P_{sw} grows (Ostapenko and Maltsev, 1998), thus leading to the current enhancement.

Tsyganenko (1996) when developing the magnetic field model T96 used the same database as we did. However, the day-night asymmetry in that model is insignificant. It is so because of some unrealistic assumptions that the T96 is based on. In particular, only weak day-night asymmetry of the ring current was postulated. The latest model T02 by Tsyganenko (2002a, b) is more accurate in this respect. We have calculated the electric currents flowing in the near-equatorial ($-3 R_E < z < 3 R_E$) layer for these models. The result is shown in Fig. 5 for moderate activity: $D_{st} = -16$ nT,

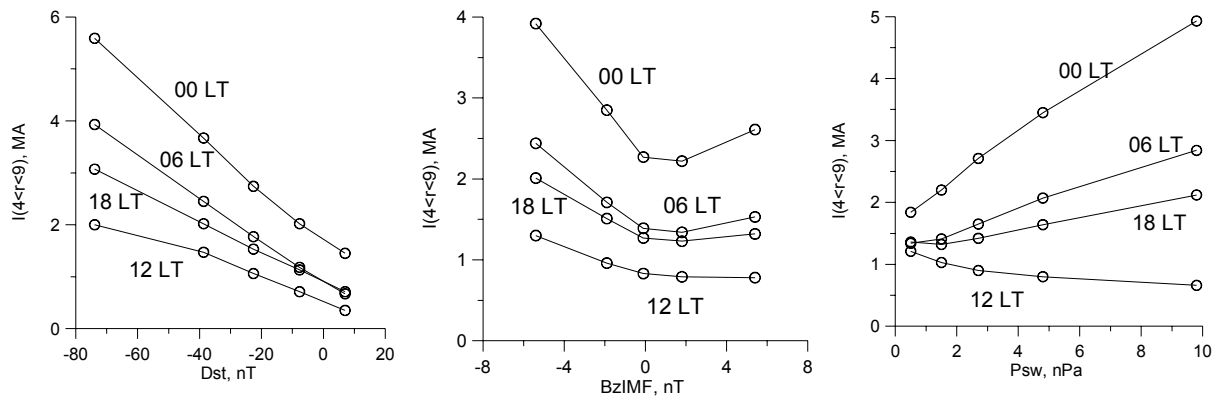


Fig. 6. The same as in Fig. 3 but for the model by Tsyganenko (2002a, b).

$P_{sw}=3$ nPa, $B_zIMF=0$. Figure 6 shows the total electric current at distances from 4 to $9 R_E$ for four local times following from the model T02. The curves have been calculated under geophysical conditions listed in Table 1. Comparison with Fig. 3 shows that the model is quite adequate to observations, manifesting strong day-night asymmetry. Instead of Eqs. (3)–(8), we obtained the following approximations for the ring current:

$$I_{\text{night}} = 1.66 - 0.047 D_{st} ,$$

$$I_{\text{noon}} = 0.57 - 0.020 D_{st} ,$$

$$I_{\text{night}} = 2.25 - 0.31 B_s ,$$

$$I_{\text{noon}} = 0.81 - 0.09 B_s ,$$

$$I_{\text{night}} = 1.75 + 0.33 P_{sw} ,$$

$$I_{\text{noon}} = 1.12 - 0.05 P_{sw} .$$

A comparison of these relations with Eqs. (3)–(8) shows their strong resemblance. The major difference is that the T02 model yields a contribution factor ~ 1.5 greater of the symmetrical ring current to D_{st} , as compared to expression (3). Thus, according to the T02 model, the contribution of the symmetrical ring current to D_{st} is $\sim 40\%$. The discrepancy between our results and those of T02 can be due to the fact that Tsyganenko (2002a) made some hypotheses concerning a possible geometry of the electric currents in the magnetosphere. As a result, the dayside current in the T02 can be overestimated, as was the case in T96. Comparatively large residual error $RES=28\%$ indicates that the approximation given by the T02 in the disks of $\rho < 10 R_E$, $2 < |z| < 4 R_E$ is not quite accurate. Our approximation is somewhat better. When dividing the whole data set into five D_{st} ranges, we get $RES=24\%$.

As seen from Fig. 1, the azimuthal electric current is rather symmetrical in the dawn-dusk direction, with no tendency for the dawn-dusk asymmetry to grow with growing activity. In contrast, a strong dawn-dusk asymmetry with an intense duskside partial ring current was obtained by Tsyganenko et al. (2003) for 37 major magnetic storms

($-65 \geq D_{st_{\min}} \geq 318$ nT). It is difficult to say whether this result follows directly from the measurements or the model infers the duskside location of the partial ring current a priori.

5 Conclusions

Magnetic data processing in the near-equatorial ($-3 R_E < z < 3 R_E$) layer shows that the longitudinal distribution of the westward electric current flowing in the inner magnetosphere (at radial distances from 4 to $9 R_E$) is quite asymmetric in the day-night direction, with the nightside current intensity being several times larger than the dayside one. It is the solar wind dynamic pressure and D_{st} that mostly control the nightside ring current intensity. The dawn-dusk asymmetry is rather weak. The radial distribution is not very sensitive to either geomagnetic activity or solar wind parameters, with the current maximum located at $5-7 R_E$. The dayside current can be considered as the symmetrical ring current. Its contribution to D_{st} is estimated as 27%. The contribution of the partial ring current, together with the nearest part of the cross-tail current flowing at distances $< 9 R_E$, is $\sim 29\%$.

Acknowledgements. This work was supported by the Russian Basic Research Foundation (grants 03-05-65379 and 03-05-20003-BNTS) and by the Division of Physical Sciences of the Russian Academy of Sciences (program DPS-16).

Topical Editor T. Pulkkinen thanks two referees for their help in evaluating this paper.

References

- Daglis, I. A., Thorne, R. M., Baumjohann, W., and Orsini, S.: The terrestrial ring current: Origin, formation, and decay, *Rev. Geophys.*, 37, 407–438, 1999.
- De Michelis, P., Daglis, I. A., and Consolini, G.: An average image of proton plasma pressure and of current systems in the equatorial plane derived from AMTE/CCE-CHEM measurements, *J. Geophys. Res.*, 104, 28 615–28 624, 1999.
- Dremukhina, L. A., Feldstein, Y. I., Alexeev, I. I., Kalegaev, V. V., and Greenspan, M. E.: Structure of the magnetospheric magnetic

- field during magnetic storms, *J. Geophys. Res.*, 104, 28 351–28 360, 1999.
- Fairfield, D. H., Tsyganenko, N. A., Usmanov, A. V., and Malkov, M. V.: A large magnetosphere magnetic field database, *J. Geophys. Res.*, 99, 11 319–11 326, 1994.
- Frank, L. A.: On the extraterrestrial ring current during geomagnetic storms, *J. Geophys. Res.*, 72, 3753–3767, 1967.
- Greenspan, M. E. and Hamilton, D. C.: A test of the Dessler-Parker-Sckopke relation during magnetic storms, *J. Geophys. Res.*, 105, 5419–5430, 2000.
- Häkkinen, L. V. T., Pulkkinen T. I., Nevanlinna H., Pirjola R. J., and Tanskanen, E. I.: Effects of induced currents on D_{st} and on magnetic variations at midlatitude stations, *J. Geophys. Res.*, 107(A1), doi:10.1029/2001JA900130, 2002.
- Hamilton, D. C., Gloeckler, G., Ipavich, F. M., Studemann, W., Wilken, B., and Kremser, G.: Ring current development during the great geomagnetic storm of February 1986, *J. Geophys. Res.*, 93, 14 343–14 355, 1988.
- Iijima, T. and Potemra, T. A.: The amplitude distribution of field-aligned currents at northern high latitudes observed by TRIAD, *J. Geophys. Res.*, 81, 2165–2174, 1976.
- Iijima, T., Potemra, T. A., and Zanetti, L. J.: Large-scale characteristics of magnetospheric equatorial currents, *J. Geophys. Res.*, 95, 991–999, 1990.
- Kalegaev, V. V., Alexeev, I. I., Feldstein, Y. I., Gromova, L. I., Grafe, A., and Greenspan, M.: Magnetic flux in the magnetotail lobes and the dynamics of D_{st} disturbances during magnetic storms (in Russian), *Geomagnetism and Aeronomy*, 38 (3), 10–16, 1998.
- Korth, A. and Friedel, R. H. W.: Dynamics of energetic ions and electrons between $L = 2.5$ and $L = 7$ during magnetic storms, *J. Geophys. Res.*, 102, 14 113–14 122, 1997.
- Langel, R. A. and Estes, R. H.: Large-scale, near-field magnetic fields from external sources and the corresponding induced internal field, *J. Geophys. Res.*, 90, 2487–2494, 1985.
- Lui, A. T. Y. and Hamilton, D. C.: Radial profiles of quiet time magnetospheric parameters, *J. Geophys. Res.* 97, 19 325–19 332, 1992.
- Lui, A. T. Y., McEntire, R. W., and Krimigis, S. M.: Evolution of the ring current during two geomagnetic storms, *J. Geophys. Res.*, 92, 7459–7470, 1987.
- Ostapenko, A. A. and Maltsev, Yu. P.: Three-dimensional magnetospheric response to variations in the solar wind dynamic pressure, *Geophys. Res. Lett.*, 25, 261–263, 1998.
- Ostapenko, A. A. and Maltsev, Yu. P.: LT and D_{st} dependence of the ring current, Proc. of the 26th Annual Seminar “Physics of Auroral Phenomena”, Apatity, 25–28 February, 2003, 83–86, 2003.
- Smith, P. H. and Hoffman, R. A.: Ring current particle distribution during the magnetic storm on December 16–18, 1971, *J. Geophys. Res.*, 78, 4731–4737, 1973.
- Spence, H. E., Kivelson, M. G., Walker, R. J., and McComas, D. J.: Magnetospheric plasma pressure in the midnight meridian: Observation from 2.5 to 35 R_E , *J. Geophys. Res.*, 94, 5264–5272, 1989.
- Terasawa, T., Fujimoto, F., T. Mukai, Shinohara, I., Saito, Y., Yamamoto, T., Machida, S., Kokubun, S., Lazarus, A. J., Steinberg, J. T., and Lepping, R. P.: Solar wind control of density and temperature in the near-Earth plasma sheet: WIND/Geotail collaboration, *Geophys. Res. Lett.*, 24, 935–938, 1997.
- Tsyganenko, N. A.: Effects of the solar wind conditions on the global magnetospheric configuration as deduced from data-based field models, in: Proc. of the Third International Conference on Substorms (ICS-3), Versailles, France, 181–185, 1996.
- Tsyganenko, N. A.: A model of the near magnetosphere with a dawn-dusk asymmetry, 1, Mathematical structure, *J. Geophys. Res.*, 107 (A8), doi10.1029/2001JA000219, 2002a.
- Tsyganenko, N. A.: A model of the near magnetosphere with a dawn-dusk asymmetry, 2, Parameterization and fitting to observations, *J. Geophys. Res.*, 107 (A8), doi10.1029/2001JA000220, 2002b.
- Tsyganenko, N. A., Singer, H. J., and Kasper, J. C.: Storm-time distortion of the inner magnetosphere: How severe can it get? *J. Geophys. Res.*, 108 (A5), doi10.1029/2002JA009808, 2003.
- Turner, N. E., Baker, D. N., Pulkkinen, T. I., Roeder, J. L., Fennell, J. F., and Jordanova, V. K.: Energy content in the storm time ring current, *J. Geophys. Res.*, 106, 19 149–19 156, 2001.